J. theor. Biol. (2000) **203,** 177–186
doi:10.1006/jtbi.2000.1075, available online at http://www.idealibrary.com on IDEAL®

A Dynamical Model for the Growth and Size Distribution of Multiple Metastatic Tumors

K. Iwata*†, K. Kawasaki‡ and N. Shigesada§

**Department of Oncoradiology, Nara Medical University, Nara* 634-0813, *Japan*, ‡*Department of Knowledge Engineering and Computer Sciences, Doshisha University, Kyo-tanabe* 610-0321, *Japan and* §*Department of Information and Computer Sciences, Nara Women's University, Nara* 630-8506, *Japan*

(*Received on* 4 *March* 1999, *Accepted on* 29 *December* 1999)

Metastasis is the spread of tumors culminating in the establishment of one or more secondary tumors at remote sites. In deciding the best treatment for cancer therapy, estimations of the colony size of metastatic tumors and predictions of the future spread of colonies are needed. A dynamical model for the colony size distribution of multiple metastatic tumors is presented here. The dynamics is described by equations that incorporate both the colonization by metastasis and the growth of each colony. When the colony growth is subject to the Gompertz function, the explicit solution obtained tends to an asymptotic stable distribution that shows a monotonically decreasing or U-shaped pattern according to the values of clinically significant parameters, such as the colonization coefficient and the fractal dimension of blood vessels. This predicted colony size distribution agrees well with successive data of a clinically observed size distribution of multiple metastatic tumors of liver cancer. The combined analysis of the theoretical colony size distribution and clinical data will give useful information on the diagnosis and the therapy for cancer patients.

1. Introduction

In some rapidly disseminating tumors, multiple colonizations of the tumor cells occur at a high frequency to form metastatic tumors (clinically called daughter nodules) within one host organ or more, such as the liver, lungs and brain. Multiple metastasis is one of the major problems that confront the cancer clinician since the spread of malignant tumors prevents successful treatment by a simple excision of the primary tumor (Evans, 1991; Mareel *et al*., 1991). Recently, developments in clinical imaging techniques have made it easier to measure the size of tumors or to estimate the distribution of blood vessels in tumors for each patient (Ohishi *et al*., 1998). However, these metastases, perhaps starting from only one or a few cells, may not be immediately detected even with modern clinical diagnostic techniques (Poste & Fidler, 1980; Nicolson & Custead, 1982; Schmitz *et al*., 1997). This raises the need for a mathematical model simulating the metastasis.

The growth characteristics of tumors and their related metastatic processes have been analysed by statistical or stochastic approaches (Bartoszynski, 1987; Klein & Bartoszynski, 1991; Kimmel & Flehinger, 1991; Yorke *et al*., 1993; Boucher *et al*., 1998; Yakovlev *et al*., 1999). In

† Author to whom correspondence should be addressed. E-mail: iwata@lisboa.ics.nara-wu.ac.jp

0022–5193/99/060177 + 10 $35.00/0

particular, Hart *et al.* (1998) have theoretically predicted static size distributions of metastatic tumors, and have compared them with clinical data from large screening trials. However, dynamical models for the colony size distribution of multiple metastatic tumors have scarcely been studied. Here we develop a model to estimate the number of tumors below the imaging detectability limit, and to quantitatively predict the future behavior of metastases in an individual patient. The behavior of the explicit solution obtained for the colony size distribution is compared with that successively measured by computed tomography (CT) images of a patient with hepatocellular carcinoma in the liver. The clinical applicability and importance of the theoretical colony size distribution based on the data of an individual patient are discussed.

2. The Mathematical Model

Metastases are widely accepted to arise from linked, sequential steps involving multiple host-tumor interactions (Nicolson & Custead, 1982; Talmadge *et al.*, 1982; Liotta *et al.*, 1983; Schirrmacher, 1985; Nicolson, 1985). To formulate the process of metastases, we consider an idealized case in which a primary tumor is generated from a single cell at time $t = 0$ and grows at rate $g(x)$ per unit time, where x denotes the tumor size represented by the number of cells in the tumor. The growing tumor emits metastatic single cells at rate $\beta(x)$. Each metastatic cell develops into a new tumor, which also grows at rate $g(x)$ and emits new nuclei of metastasis just as the primary tumor does (Hoover & Ketcham, 1975; Talmadge *et al.*, 1982).

Let $\rho(x, t)$ represent the colony size distribution of metastatic tumors with cell number x at time t. Namely, $\rho(x, t)\,\mathrm{d}x$ means the number of metastatic tumors whose sizes range from x to $x + \mathrm{d}x$ at time t. Here, we focus on a case in which the nuclei of colonization are located far enough from each other so that their ranges do not overlap for a long period of time. We further assume that tumors are not eliminated by treatments or natural death. Then the dynamics of the colony size distribution is described by the following von Foerster equation (Shigesada *et al.*, 1995; Shigesada & Kawasaki, 1997; see Appendix A for derivation)

$$\frac{\partial \rho(x,\ t)}{\partial t} + \frac{\partial g(x)\rho(x,\ t)}{\partial x} = 0 \tag{1a}$$

with the initial and boundary conditions,

$$\rho(x,\ 0) = 0, \tag{1b}$$

$$g(1)\,\rho(1,\ t) = \int_1^\infty \beta(x)\,\rho(x,\ t)\,\mathrm{d}x + \beta(x_p(t)). \tag{1c}$$

Equation (1b) means that initially no metastatic tumor exists. Equation (1c) indicates that the number of metastatic single cells newly created per unit time at time t [the left-hand side (l.h.s.) term] is the total rate of occurrence of metastases due to metastatic tumors and the primary tumor [corresponding to the first and second terms of the right-hand side (r.h.s.)]. $x_p(t)$ represents the number of cells in the primary tumor at time t, which, by definition, is given by the solution of

$$\frac{\mathrm{d}x_p}{\mathrm{d}t} = g(x_p), \quad x_p(0) = 1. \tag{1d}$$

In the following analysis, we adopt the Gompertzian growth rate for $g(x)$,

$$g(x) = ax \log \frac{b}{x}, \tag{2}$$

where a is the growth rate constant and b is the tumor size at the saturated level. The Gompertzian growth rate has been well documented to cover a wide range of empirical data (Laird, 1965; Archambeau *et al.*, 1970; Akanuma, 1978; Gyllenberg & Webb, 1990). Substituting eqn (2) into eqn (1d) and solving the resultant equation, we obtain the number of cells in the primary tumor as a function of time

$$x_p(t) = b^{1 - \mathrm{e}^{-at}}. \tag{3}$$

There have been alternative growth functions such as the exponential growth and power-law growth (Hart *et al.*, 1998). The following analysis is applicable to these growth rates as described in Discussion.

For the colonization rate $\beta(x)$, we adopt the following form:

$$\beta(x) = mx^{\alpha}, \tag{4}$$

where m is the colonization coefficient and α is the fractal dimension of blood vessels infiltrating the tumor (Weidner *et al.*, 1991; Horak *et al.*, 1992; Weinstat-Saslow & Steeg, 1994; Folkman, 1995; Meitar *et al.*, 1996). Equation (4) mechanistically implies that the rate of metastasis from a tumor with size x is proportional to the number of tumor cells in contact with blood vessels, which provide channels for cell dispersal (Poste & Fidler, 1980; Schirrmacher, 1985). The parameter α, called the fractal dimension, expresses how the blood vessels geometrically distribute in or on a tumor (Gazit *et al.*, 1997; Braish & Jain, 1998). For example, when the tumor vascularity is superficial, that is, the blood vessels distribute on the surface of the tumor, the fractal dimension α is assigned to be $\frac{2}{3}$, because the surface area of the tumor is proportional to $x^{2/3}$. On the other hand, when the blood vessels homogeneously distribute in the whole tumor, α is 1. In this paper, the fractal dimension α is dealt with as an unknown parameter, and is determined by fitting the theoretical colony size distribution to clinical data.

To analytically solve eqn (1) with eqns (2)–(4), we employ the Laplace transformation method to obtain the explicit solution as (see Appendix B for derivation):

$$\rho(x, t) = \frac{a}{mb^{\alpha}\log b}\frac{1}{x}\sum_{k=1}^{\infty} e^{a\lambda_k t}\left(1 - \frac{\log x}{\log b}\right)^{(\lambda_k - 1)}\frac{1}{c(\lambda_k)}$$

$$\text{for } 1 \leqslant x < x_p(t), \tag{5}$$

where $c(\lambda_k) = \sum_{n=0}^{\infty} [(-\alpha\log b)^n]/[n!(\lambda_k + n)^2]$. λ_ks are the solutions of the following equation:

$$\frac{a}{m}\lambda_k = F(1, \lambda_k + 1; \alpha\log b), \tag{6}$$

where

$$F(\alpha, \gamma; z) = \sum_{n=0}^{\infty}\frac{\alpha(\alpha+1)\cdots(\alpha+n-1)}{\gamma(\gamma+1)\cdots(\gamma+n-1)}\frac{z^n}{n!}, \tag{7}$$

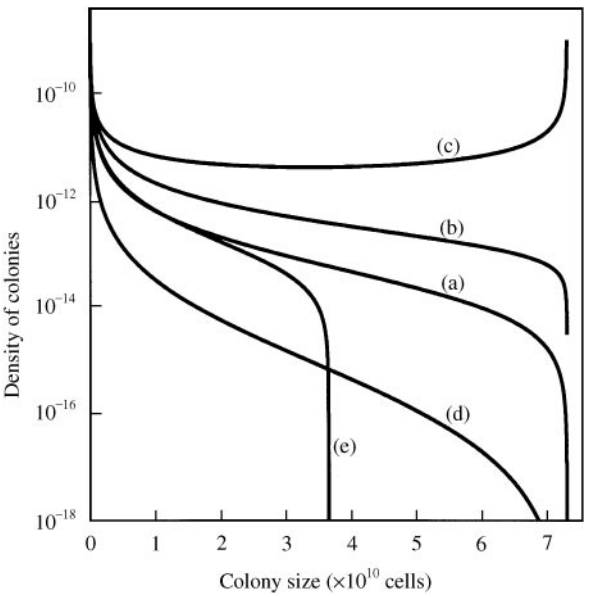

FIG. 1. Asymptotic colony size distributions with the Gompertz growth for varying parameter values. All the distributions are normalized to unity. (a) $a = 0.00286$, $b = 7.3 \times 10^{10}$, $m = 5.3 \times 10^{-8}$, $\alpha = 0.663$. For the remaining curves, one of the parameters is changed from those used in (a) as follows: (b) $a = 0.0143$; (c) $\alpha = 0.4$; (d) $\alpha = 0.8$; (e) $b = 3.65 \times 10^{10}$. Parameters values in (a) are taken from those obtained for a particular patient dealt with in Section 3.

which is the confluent hypergeometric function of Kummer (Whittaker & Watson, 1962). Equation (6) has a unique positive dominant root λ_1. This means that the term associated with λ_1 in the summation of the r.h.s. of eqn (5) represents an asymptotic tumor size distribution at a sufficiently long time, which is proportional to $(1 - \log x/\log b)^{\lambda_1 - 1}/x$. If $\lambda_1 > 1$, the asymptotic tumor size distribution becomes a monotonically decreasing function of x. If $\lambda_1 < 1$, on the other hand, the asymptotic distribution becomes U-shaped. Condition $\lambda_1 > 1$ is explicitly given by $m > a\alpha\log b/(b^{\alpha} - 1)$ and vice versa, because (6) for $\lambda_1 = 1$ is rewritten as $a/m = (b^{\alpha} - 1)/(\alpha\log b)$. Figure 1 demonstrates how the shape of the colony size distribution varies with these parameter values.

3. A Clinical Application

To evaluate the practical applicability of the model, multiple metastatic tumors in a liver with a hepatocellular carcinoma as a primary tumor

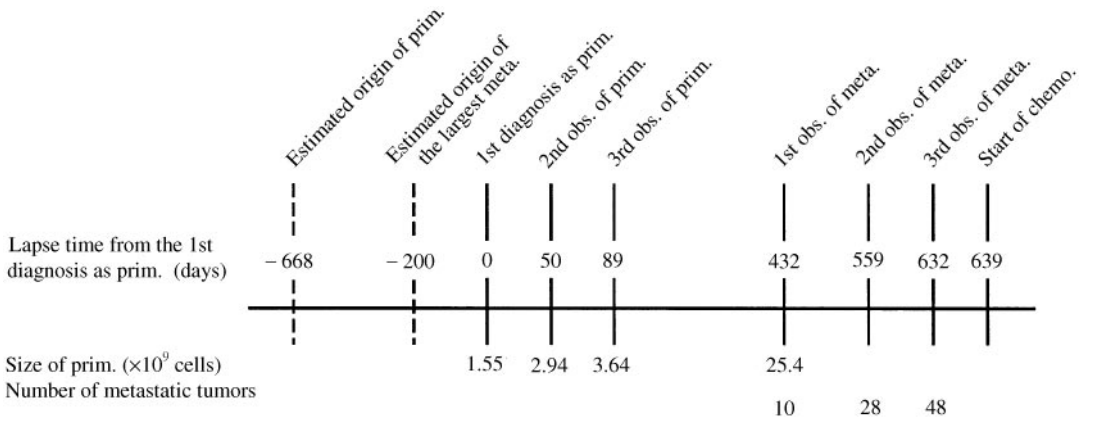

FIG. 2. Clinical history of a patient with a hepatocellular carcinoma as a primary tumor and multiple metastatic tumors in the liver. Although the patient was first treated with mild transcatheter arterial embolization (TAE), the metastasis could not be controlled. The progression of metastasis was surveyed by three successive CT imagings until the chemotherapy was started. By our simulation, the estimated times of inception of the primary tumor and the largest metastatic tumor were 668 days and 200 days prior to the first diagnosis of the primary tumor, respectively. Abbreviations: prim. = primary tumor; meta. = metastases; chemo. = chemotherapy.

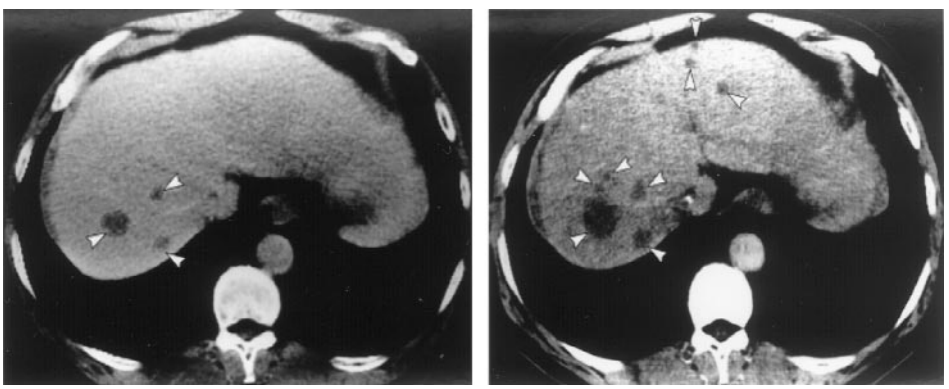

FIG. 3. Contrast-enhanced X-ray computed tomographies (CT) of the liver with multiple metastatic tumors. The left and right panels were CT images scanned on 432 days and 559 days after the first diagnosis of the primary tumor, respectively. Several metastatic tumors are seen as low attenuated areas (arrowheads indicate typical ones). The number of tumors and the size of each tumor observed within the right tomography increased compared to those within the left tomography. In this work, the sizes of all tumors detectable within the whole liver by using all the CT slices were measured.

were retrospectively surveyed. The clinical history is shown in Fig. 2. The sizes of the tumors were measured by using X-ray CT images (Fig. 3) or subtracted angiographies. In order to study the behavior of natural metastasis with minimal artificial modifications, we reviewed three sequential CT images at different times before starting the patient's chemotherapy. The numbers of metastatic tumors detected were 10, 28 and 48 on 432 days, 559 days and 632 days after the first diagnosis as a primary tumor, respectively. Each tumor colony was observed to grow at rates consistent with eqn (2). Figure 4(a) shows the cumulative number of metastases plotted against the tumor colony size for successive dates of observation. The theoretical cumulative distributions are generated by integrating eqn (5) from x to infinity (i.e. $N(x, t) = \int_x^\infty \rho(x, t)\,dx$). The values of the four unknown parameters in our model and the time of the primary tumor inception were determined, by fitting the theoretical curve to the observed cumulative size distribution through the least-squares regression. The results were: $a = 0.00286\ \text{day}^{-1}$, $b = 7.3 \times 10^{10}$ cells, $\alpha = 0.663$, $m = 5.3 \times 10^{-8}\,(\text{cell day})^{-1}$ and the time of the primary inception was 668 days prior to the first diagnosis. As seen in Fig. 4(a), the whole series of clinical data fit well with the

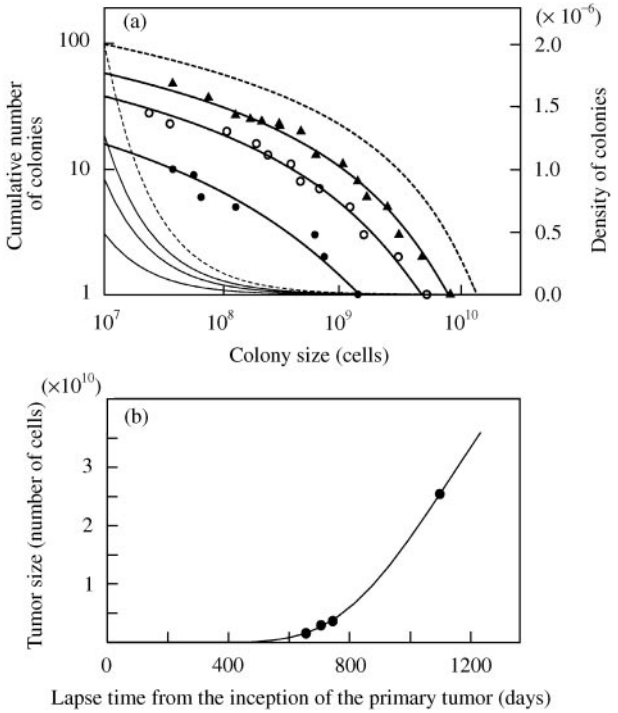

FIG. 4. Changes in the size distribution of tumors with progression of metastasis of a hepatocellular carcinoma. (a) The cumulative number of tumors as a function of the colony size were observed at three successive times after the first diagnosis of the primary tumor: day 432, ●; day 559, ○; day 632, ▲. The thick curves are theoretical cumulative distributions. The thin lines are the colony size distributions (5) for the corresponding thick curves. The thick and thin dashed lines indicate predicted states of metastasis at 732 days after the first diagnosis (for details, see text). The number of tumors for the left-most data point at each observation time indicates the total number of tumors detectable by using CT images. The volume of the tumor was estimated by assuming that the shape of the tumor was a spheroidal ellipsoid. A tumor of $1\,\mathrm{mm}^3$ was assumed to contain 10^6 cells (Akanuma, 1978). (b) The theoretical Gompertz growth compared with the observed growth data of the primary tumor. The left-most data point indicates the size of the primary tumor at the first diagnosis. The theoretical curve is given by $b^{1-\mathrm{e}^{-at}}$, where $a = 0.00286$ and $b = 7.3 \times 10^{10}$.

theoretical curves generated with these parameter values. Furthermore, the theoretical Gompertz growth $x_p(t) = b^{1-\mathrm{e}^{-at}}$ assigned with these parameter values agrees well with the growth data of the primary tumor [see Fig. 4(b)]. It is also concluded that the asymptotic size distribution of metastatic tumors is monotonically decreasing because the above-noted criterion, $m > a\,\alpha \log b/(b^{\alpha} - 1)$, is met with these parameters [see the thin curves in Fig. 4(a)].

From this analysis, we can draw a number of predictions as follows: (1) The future behavior of metastasis can be simulated as shown by the dashed lines in Fig. 4(a). (2) By extrapolating the theoretical curve for the cumulative tumor number to infinitesimal sizes, we can estimate the number of tumors smaller than a few millimeters, the lower limit of size detectable with modern clinical diagnostic techniques (Schmitz *et al.*, 1997). Thus, the total estimated numbers of tumors including single cells are 135, 263, 396 and 712 on 432 days, 559 days, 632 days and 732 days after the first diagnosis of the primary tumor, respectively. (3) Since the fractal dimension of blood vessels is close to $\frac{2}{3}$ ($\alpha = 0.663$), the tumor vascularity is supposed to be nearly superficial. This is confirmed by CT imaging as well as subtracted angiography (data not shown). (4) Furthermore, our model for the colony size distribution allows us to estimate the times of origin of metastases. For example, the growth of the largest metastatic tumor is supposed to have started 200 days prior to the first diagnosis of the primary tumor.

4. Discussion

Tumors that are actively generating multiple metastases are beyond any form of therapeutic control. Imaging techniques such as X-ray CT, magnetic resonance imaging (MRI), and ultrasonography (US) continue to be improved for use in clinical cancer diagnoses. The precise size of cancer cell colonies can be measured with three-dimensional high-spatial resolution-imaging techniques (Choi *et al.*, 1995). However, even the most up-to-date imaging techniques cannot reliably detect colonies smaller than a few millimeters in size. The presence of undetectable metastasis compounds the clinical problem, for it is difficult to treat what cannot be recognized. The dynamical model presented here can be used to estimate the number of colonies below the imaging detectability limit, and to predict the future behavior of metastasis.

Our model assumes that colonization begins from a single cell. This scenario is consistent with the experimental observation that metastases are clonal in origin and result from single cells (Talmadge *et al.*, 1982; Talmadge & Zbar, 1986).

Equation (1c) indicates that each colony has the possibility of metastasizing, and that the probability of metastasis depends on the colony size and the tumor vascularity. Experimental evidence for the ability of metastases to metastasize has been reported with the use of parabiotic experiments in mice (Hoover & Ketcham, 1975). Previously, Yorke *et al.* (1993) presented a different model for the metastatic process: as a primary tumor grows, mutations take place to impart metastatic potential to some cells. This model was originally proposed to explain the development of drug resistance in tumors by Goldie & Coldman (1979). However, it did not address the secondary dissemination of metastases.

We assumed that only the tumor cells contacting blood vessels can emit new nuclei of metastatic tumors, which are spread via the blood stream. This assumption is indirectly supported by several experiments. For example, animal experiments have shown that liver metastases occurred only in animals with vascular invasion into primary lesions (Tabuchi *et al.*, 1991). Another study found that the number of circulating tumor cells was correlated with the density of tumor blood vessels and also with the incidence of metastasis (Loitta *et al.*, 1976).

In this study it is assumed, to avoid overparametrization, that the host–tumor interaction is spatially homogeneous, and that there is no fusion between colonies, which are well separated from each other. With visualization of tumors, this can be confirmed by the uniform geometric growth of colonies in the host organ. If these conditions hold, it is expected that the shape of each tumor is spheroid, and that each colony grows at the same growth rate. In fact, multiple metastatic nodules (colonies) in the same patient have been reported to grow at similar fixed rates, although wide variations in the growth rate occur between patients. (Archambeau *et al.*, 1970; Joseph *et al.*, 1971; Akanuma, 1978).

As for the tumor growth, the exponential function and the Gompertz function have been well documented (Collins *et al.*, 1956). Recently, the power-law growth was proposed, based on extensive clinical data from large mammography screening trials (Hart *et al.*, 1998). Although we used the Gompertzian growth rate, the general framework of our model is independent of this choice; calculations can be carried out using other functions for $g(x)$. When tumor growth is subject to the exponential or power-law growth, eqn (1) can similarly be solved by the Laplace transformation method used in the case of Gompertz growth. The results are briefly summarized below.

The exponential growth rate is given by

$$g(x) = ax,$$

where the parameter a is the growth rate constant.

The colony size distribution is explicitly obtained as

$$\rho(x, t) = \frac{m}{a} x^{-\alpha-(m/a)-1} e^{(a\alpha+m)t},$$

where m and α are, respectively, the colonization coefficient and the fractal dimension, as defined before.

The power-law growth rate is given by

$$g(x) = ax^{1-\gamma} \quad \text{for } 0 \leqslant \gamma \leqslant 1,$$

where the parameter a is the growth rate constant and the exponent γ is an indicator of the mode of tumor growth: when $\gamma = 1$, the colony growth is linear with time, and when $\gamma = 0$, the colony growth is exponential with time. Although the explicit solution for this case is very complicated, its asymptotic solution at a sufficiently long time is proportional to

$$\rho(x, t) \propto x^{-1+\gamma} e^{-(\lambda_1/\gamma)(x^\gamma-1)} e^{a\lambda_1 t} \quad (0 < \gamma \leqslant 1),$$

where λ_1 is a maximum real solution of equation, $1 = m/a e^{(\lambda/a\gamma)} \gamma^{\alpha/\gamma} (a/\lambda)^{(\alpha/\gamma)+1} \Gamma((\alpha/\gamma)+1, \lambda/a\gamma)$, and $\Gamma(.,.)$ is the second incomplete gamma function.

Different types of growth rates predict different colony size distributions. Both the exponential growth and the power-law growth give monotonically damping distributions with infinitely extending tails after lapse of sufficient time, although the former dampens more rapidly than the latter. While the Gompertz growth exhibits a colony size distribution similar to that of the exponential growth at an early stage, the former

develops a characteristic distribution that is limited by a fixed maximum size, and varies from monotonically damping patterns to U-shaped ones depending on whether $m/a > \alpha \log b/(b^{\alpha} - 1)$ or vice versa. Namely, the U-shape tends to arise as m/a (colonization coefficient/growth rate) increases. The data from the present clinical study fitted remarkably well with the model using the Gompertz growth in various aspects examined: time development of colony size distribution with monotonical damping, and the growth dynamics of the primary tumor.

The behavior of the colony size distribution of a tumor may change after treatment such as surgery, chemotherapy, or radiotherapy, upon which the colonization of tumor cells was reported to increase (Sandler & Hanks, 1988; Evans, 1991; Mareel *et al*., 1991). Thus, "artificial metastasis" may be distinguished from spontaneous metastasis by the pattern of their size distribution. Our model may also be used to make the distinction between metastases and multiple primary tumors such as AIDS-associated Kaposi sarcoma, or those induced by chemical carcinogens. Considerations of such possible etiologic conditions will lead to more exact diagnoses.

Our mathematical model is specified by the tumor growth rate, the fractal dimension of blood vessels associated with the tumor cells, and the colonization rate. These clinically significant parameters can also exhibit wide variations among individual patients. For example, in adenocarcinoma of the lung, the doubling time was reported to range from 15 to 960 days (Stanley *et al*., 1978). A metastasis experiment with nude mice showed that the colonization coefficient varied markedly among the transfected cell types (Lewis *et al*., 1996). A clinical study reported that metastatic potentials could vary widely even among cancers of the same general histological and anatomic location (Lindeberg, 1972). Since we cannot always know the values of these parameters for every patient, statistical inferences based on a large clinical data set of patients will play important roles in deciding a reasonable diagnosis and therapy for the patient (Bartoszynski, 1987; Klein & Bartoszynski, 1991; Yorke *et al*, 1993; Yakovlev & Tsodikov, 1996; Hart *et al*., 1998). For example, Kimmel & Flehinger (1991) studied the relationship between the size of primary tumor and the occurrence of metastases by non-parametric statistics. However, with recent developments of imaging techniques, more exact information on individual patients is becoming available. Thus, the time is ripe to develop individual-based models and to apply them for therapy. A quantitative prediction of metastasis is critical in estimating the efficacy of therapy for metastatic disease. The effect of chemotherapy largely depends on the tumor size or vascularity, since there is a limit to the diffusion of a drug within the tumor (Sutherland, 1988; Durand, 1989). Our explicit solution should be potentially useful for designing specifically tailored cancer therapies for individual patients, because the size distribution according to individual clinical data can be easily calculated with a personal computer.

We thank Dr Yasutaka Shibuya of the Department of Mathematics, University of Minnesota and the members of the Department of Central Radiology, Nara Medical University, for useful discussions.

REFERENCES

AKANUMA, A. (1978). Parameter analysis of Gompertzian function growth model in clinical tumors. *Eur. J. Cancer* **14,** 681–688.

ARCHAMBEAU, J. O., HELLER, M. B., AKANUMA, A. & LUBELL, D. (1970). Biological and clinical implications obtained from the analysis of cancer growth curves. *Clin. Obstet. Gynecol.* **13,** 831–856.

BARTOSZYNSKI, R. (1987). A modeling approach to metastatic progression of cancer. In: *Cancer Modeling* (Thompsom, J. R. & Brown, B. W., eds), pp. 237–267, New York: Marcel Dekker.

BOUCHER, K., PAVLOVA, L. V. & YAKOVLEV, A. Y. (1998). A model of multiple tumorigenesis allowing for cell death: quantitative insight into biological effects of urethane. *Math. Biosci.* **150,** 63–82.

BRAISH, J. W. & JAIN, R. K. (1998). Cancer, angiogenesis and fractals. *Nature Med.* **4,** 984.

CHOI, B. I., HAN, J. K., CHO, J. M., CHOI, D. S., HAN, M. C., LEE, H. S. & KIM, C. Y. (1995). Characterization of focal hepatic tumors. Value of two-phase scanning with spiral computed tomography. *Cancer* **76,** 2434–2442.

COLLINS, V. P., LOEFFELER, R. K. & TIVEY, H. (1956). Observations on growth rates of human tumors. *Am. J. Roentgenol.* **76,** 988–1000.

DURAND, R. E. (1989). Distribution and activity of antineoplastic drugs in a tumor model. *J. Nat. Cancer Inst.* **81,** 146–152.

EVANS, C. W. (1991). *The Metastatic Cell*: *Behavior and Biochemistry*. London: Chapman & Hall.

FOLKMAN, J. (1995). Angiogenesis in cancer, vascular, rheumatoid and other disease. *Nature Med.* **1,** 27–31.

GAZIT, Y., BRAISH, J. W., SAFABAKHSH, N., LEUNING, M., BAXTER, L. T. & JAIN, R. K. (1997). Fractal characteristics of tumor vascular architecture during tumor growth and regression. *Microcirculation* **4,** 395–402.

GOLDIE, J. H. & COLDMAN, A. J. (1979). A mathematical model for relating the drug sensitivity of tumors to their spontaneous mutation rate. *Cancer Treat. Rep.* **63,** 1727–1733.

GYLLENBERG, M. & WEBB, G. F. (1990). Nonlinear structured population model of tumor growth with quiescence. *J. Math. Biol.* **28,** 671–694.

HART, D., SHOCHAT, E. & AGUR, Z. (1998). The growth law of primary breast cancer as inferred from mammography screening trials data. *Br. J. Cancer* **78,** 382–387.

HOOVER, H. C. & KETCHAM, A. S. (1975). Metastasis of metastases. *Am. J. Surg.* **130,** 405–411.

HORAK, E. R., LEEK, R., KLENK, N., LEJEUNE, S., SMITH, K., STUART, N., GREENALL, M., STEPNIEWSKA, K. & HARRIS, A. L. (1992). Angiogenesis, assessed by platelet/endothelial cell adhesion molecule antibodies, as indicators of node metastases and survival in breast cancer. *Lancet* **340,** 1120–1124.

JOSEPH, W. L., MORTON, D. L. & ADKINS, P. C. (1971). Variation in tumor doubling time in patients with pulmonary metastatic disease. *J. Surg. Oncol.* **3,** 143–149.

KIMMEL, M. & FLEHINGER, B. J. (1991). Nonparametric estimation of the size-metastasis relationship in solid cancers. *Biometrics* **47,** 987–1004.

KLEIN, J. P. & BARTOSZYNSKI, R. (1991). Estimation of growth and metastatic rates of primary breast cancer. In: *Mathematical Population Dynamics* (Arino, O., Axelrod, D. E. & Kimmel, M., eds.), pp. 397–412. New York: Marcel Dekker.

LAIRD, A. K. (1965). Dynamics of tumor growth: comparison of growth rates and extrapolation of growth curve to one cell. *Br. J. Cancer* **19,** 278–291.

LEWIS, A. M., SU, M., DOTY, J., CHEN, Y. & PARDO, F. S. (1996). Relationship between intrinsic radiation sensitivity and metastatic potential. *Int. J. Radiat. Oncol. Biol. Phys.* **34,** 103–110.

LINDEBERG, R. (1972). Distribution of cervical lymph node metastases from squamous cell carcinoma of the upper respiratory and digestive tracts. *Cancer* **29,** 1446–1449.

LIOTTA, L. A., RAO, C. N. & BARSKY, S. H. (1983). Tumour invasion and the extracellular matrix. *Lab. Invest.* **49,** 636–649.

LOITTA, L. A., SAIDEL, G. M. & KLEINERMAN, J. (1976). The significance of hematogenous tumor cell clumps in the metastic processes. *Cancer Res.* **36,** 889–894.

MAREEL, M. M., DE BAETSELIER, P. & VAN ROY F. M. (1991). *Mechanisms of Invasion and metastasis.* Boca Raton, FL: CRC Press.

MEITAR, D., CRAWFORD, S. E., RADEMAKER, A. W. & COHN, S. L. (1996). Tumor angiogenesis correlates with metastatic disease, N-myc amplification, and poor outcome in human neuroblastoma. *J. Clin. Oncol.* **14,** 405–414.

NICOLSON, G. L. & CUSTEAD, S. E. (1982). Tumor metastasis is not due to adaptation of cells to a new organ environment. *Science* **215,** 176–178.

NICOLSON, G. L. (1985). Cancer metastasis. Tumor cell and host organ properties important in metastasis to specific secondary site. *Biochim. Biophys. Acta* **948,** 175–224.

OHISHI, H., HIRAI, T., YAMADA, R., HIROHASHI, S., UCHIDA, H., HASHIMOTO, H., JIBIKI, T. & TAKEUCHI, Y. (1998). Three-dimensional power Doppler sonography of tumor vascularity. *J. Ultrasound Med.* **17,** 619–622.

POSTE, G. & FIDLER, I. J. (1980). The pathogenesis of cancer metastasis. *Nature* **283,** 139–146.

SANDLER, H. M. & HANKS, G. E. (1988). Analysis of the possibility that transurethral resection promotes metastasis in prostate cancer. *Cancer* **62,** 2622–2627.

SCHIRRMACHER, V. (1985). Cancer metastasis: experimental approaches, theoretical concepts and impacts for treatment strategies. *Adv. Cancer Res.* **43,** 1–73.

SCHMITZ, S. A., WAGNER, S., SCHUHMANN-GIAMPIERI, G., KRAUSE, W. & WOLF, K. J. (1997). Detection of focal liver lesions: CT of the hepatobiliary system with gadoxetic acid disodium, or Gd-EOB-DTPA. *Radiology* **202,** 399–405.

STANLEY, E., SHACKNEY, S. E., MCCORMIC, G. W. & CUCHURAL, G. J. (1978). Growth rate patterns of solid tumors and their relation to responsiveness to therapy. *Ann. Intern. Med.* **89,** 107–121.

SHIGESADA, N. & KAWASAKI, K. (1997). *Biological Invasions: Theory and Practice.* Oxford: Oxford University Press.

SHIGESADA, N., KAWASAKI, K. & TAKEDA, Y. (1995). Modeling stratified diffusion in biological invasions. *Am. Nat.* **146,** 229–251.

SUTHERLAND, R. M. (1988). Cell and environment interactions in tumor microregions. The multicell spheroid model. *Science* **240,** 177–184.

TABUCHI, Y., NAKAMURA, T. & SAITO, Y. (1991). Liver metastases inducedby implantaion of VX2 cancer into the gastrointesine. *J. Surg. Res.* **50,** 216–222.

TALMADGE, J. E., WOLMAN, S. R. & FIDLER, I. J. (1982). Evidence for the clonal origin of spontaneous metastasis. *Science* **217,** 361–363.

TALMADGE, J. E. & ZBAR, B. (1986). Clonality of pulmonary metastases from the bladder 6 subline of the B16 melanoma studied by southern hybridization. *J. Natl. Cancer Inst.* **78,** 315–320.

WEIDNER, N., SEMPLE, J. P., WELCH, W. R. & FOLKMAN, J. (1991). Tumor angiogenesis and metastasis-correlation in invasive breast carcinoma. *N. Engl. J. Med.* **324,** 1–8.

WEINSTAT-SASLOW, D. & STEEG, P. S. (1994). Angiogenesis and colonization in the tumor metastatic process: basis and applied advances. *FASEB J.* **8,** 401–407.

WHITTAKER, E. T. & WATSON, G. N. (1962). *A Course of Modern Analysis* 4th Edn. Cambridge: Cambridge University Press.

YAKOVLEV, A. Y. & TSODIKOV, A. D. (1996). *Stochastic Models of tumor Latency and their Biostatistical Applications.* Singapore: World Scientific Publishers.

YAKOVLEV, A. Y., BOUCHER, K. & DISARIO, J. (1999). Modeling insight into spontaneous regression of tumors. *Math. Biosci.* **155,** 45–60.

YORKE, E. D., FUKS, L., NORTON, W., WHITMORE, W. & LING, C. C. (1993). Modeling the development of metastases from primary and locally recurrent tumors: comparison with a clinical data base for prostatic cancer. *Cancer Res.* **53,** 2987–2993.

APPENDIX A

Derivation of eqn (1a)

Since we assume that there is no loss of tumors by treatments or death, a tumor of size x will

grow to a tumor of size $x + g(x)\,dt$ after a period of dt. Therefore, the following equation holds:

$$\rho(x, t)\,\Delta x = \rho(x + g(x)\,\Delta t,\ t + \Delta t)\{\Delta x + g(x + \Delta x)\,\Delta t - g(x)\,\Delta t\}.$$

By expanding the r.h.s. with respect to Δx and Δt, we obtain

$$\rho(x,t)\Delta x = \{\rho(x,t) + \rho_x(x,t)g(x)\,\Delta t + \rho_t(x,t)\,\Delta t + \cdots\}\{\Delta x + (g(x) + g_x(x)\,\Delta x + \cdots)\,\Delta t - g(x)\,\Delta t\}.$$

Rearranging this equation and letting $\Delta x \to 0$ and $\Delta t \to 0$ gives the differential equation:

$$\frac{\partial \rho(x,t)}{\partial t} + \frac{\partial g(x)\rho(x,t)}{\partial x} = 0.$$

APPENDIX B

Derivation of Analytic Solution of eqn (1)

By applying the Laplace transformation to eqns (1a) with (1b), we have

$$s\tilde{\rho}(x,s) + \frac{\partial}{\partial x}(g(x)\tilde{\rho}(x,s)) = 0,$$

which is solved as

$$\tilde{\rho}(x,s) = \frac{F(s)}{g(x)} e^{-s\int_1^x du/g(u)}, \tag{B.1}$$

where $F(s)$ is an arbitrary function of s.

We next apply the Laplace transformation to eqn (1c), and obtain

$$g(1)\tilde{\rho}(1,s) = \int_1^\infty \beta(x)\tilde{\rho}(x,t)\,dt + \int_0^\infty \beta(x_p(t))e^{-st}\,dt. \tag{B.2}$$

By substituting eqn (B.1) into eqn (B.2) and rearranging the resultant equation, we get

$$\tilde{\rho}(x,s) = \frac{B_p(s)G(x,s)}{1 - \int_1^\infty \beta(x)G(x,s)\,dx}, \tag{B.3}$$

where

$$B_P(s) = \int_0^\infty \beta(x_p(t))\,e^{-st}\,dt$$

and

$$G(x,s) = \frac{1}{g(x)} e^{-s\int_1^x du/g(u)}.$$

$Bp(s)$ and $G(x,s)$ are substituted, respectively, by x_p as given by eqn (3) and the Gompertz growth rate, $g(x) = ax\log(b/x)$, and integration is performed. Then we obtain,

$$B_p(s) = \int_1^\infty \beta(x)G(x,s)\,dx = \frac{m}{s}F\left(1, \frac{s}{a} + 1;\ \alpha\log b\right).$$

Thus, eqn (B.3) is rewritten as

$$\tilde{\rho}(x,s) = \frac{1}{a\log b}\frac{1}{x}\left(1 - \frac{\log x}{\log b}\right)^{(s/a)-1}\left\{-1 + \frac{s/m}{s/m - F(1, s/a + 1;\ \alpha\log b)}\right\}. \tag{B.4}$$

Applying the Laplace inverse transformation to eqn (B.4), we have

$$\rho(x,t) = \frac{1}{a\log b}\frac{1}{x}\left(1 - \frac{\log x}{\log b}\right)^{-1} \sum_{k=1}^{\infty} Res[f(s), a\lambda_k], \tag{B.5}$$

where

$$f(s) = e^{(s/a)\log[1 - (\log x)/(\log b)] + st}\left\{-1 + \frac{s/m}{s/m - F(1, s/a + 1;\ \alpha\log b)}\right\}. \tag{B.6}$$

The poles of $f(s)$, $a\lambda_k$ $(k = 1, 2, 3, \ldots)$, are the roots of

$$\frac{a}{m}\lambda_k = F(1, \lambda_k + 1; \alpha \log b).$$

Calculating the residues at these poles, we have finally

$$\rho(x, t) = \frac{a}{mb^{\alpha} \log b} \frac{1}{x} \sum_{k=1}^{\infty} e^{a\lambda_k t} \left(1 - \frac{\log x}{\log b}\right)^{(\lambda_k - 1)} \frac{1}{c(\lambda_k)}$$

$$\text{for } 1 \leqslant x < x_p(t), \tag{B.7}$$

where $c(\lambda_k) = \sum_{n=0}^{\infty} [(-\alpha \log b)^n]/[n!(\lambda_k + n)^2]$.